Computational Evaluation of Corrosion Inhibition of Four Quinoline Derivatives on Carbon Steel in Aqueous Phase

Elmi, Shirin; Foroughi, Mohammad Mehdi*[+]

Department of Chemistry, Kerman Branch, Islamic Azad University, Kerman, I.R. IRAN

Dehdab, Maryam

Young Researchers and Elite Club, Bushehr Branch, Islamic Azad University, Bushehr, I.R. IRAN

Shahidi Zandi, Mehdi

Department of Chemistry, Kerman Branch, Islamic Azad University, Kerman, I.R. IRAN

ABSTRACT: *Molecular Dynamics (MD) simulation and Density Functional Theory (DFT) methods have been used to evaluate the efficiency of four quinoline derivatives on corrosion inhibition in the aqueous phase. Some quantum chemical parameters such as hardness (η), electrophilicity (ω), polarizability (α), energy of the highest occupied molecular orbital (E_{HOMO}), energy of the lowest unoccupied molecular orbital (E_{LUMO}), electronegativity (χ), total amount of electronic charge transferred (ΔN), Total Negative Charges (TNC) on the whole of the molecule, Molecular Volume (MV), surface area and Fukui index were calculated. Molecular dynamics simulation showed a view of the dynamic evolution of the interaction energy between surface of metal and inhibitors. Results of two methods showed QUIN4 inhibitor has higher negative interactions and efficiency as compared to the other inhibitors, which was consistent with the experimental report.*

EYWORDS: *Corrosion; Quinoline Derivatives; DFT; Molecular Dynamics Simulation; Carbon Steel.*

INTRODUCTION

Carbon steel is one of the most important materials in the structure of equipment and accessories in plenty of industries and plants, because of mechanical properties, hardness, and economic aspects. However, indispensable phenomenon namely corrosion causes big damage. Nowadays, corrosion inhibition is a very important topic in research works of scientists with concerting on new organic and inorganic compounds as inhibitors [1-2]. Computational methods are sometimes prior than experimental studies and have recently found a significant role in evaluating the efficiency of inhibitors on corrosion of metals such as carbon steel. Quantum chemical calculations and molecular dynamic simulation are used as effective tools to investigate chemical properties and inhibitor-metal interactions [3-5].

In this work, the experimental data reported [6], is compared with computational inhibitory results obtained from quinoline derivatives (Fig. 1) such as

** To whom correspondence should be addressed.*

+ E-mail: mmforoughi95@yahoo.com

1021-9986/2019/1/185-200 16/$/6.06

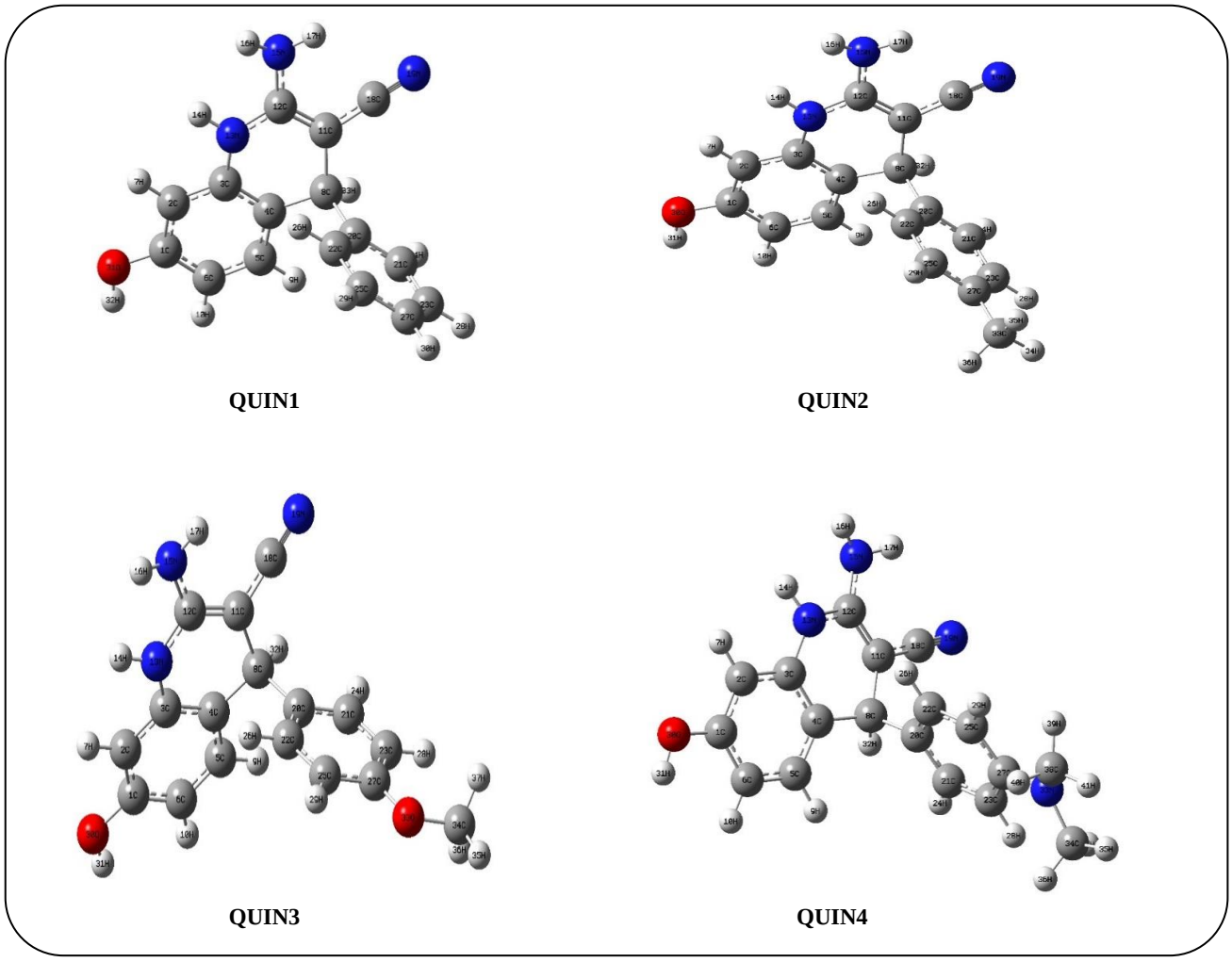

Fig. 1: The optimized structures of the studied quinoline derivatives 2-amino-7-hydroxy-4-phenyl-1,4-dihydroquinoline -3-carbonitrile (QUIN1), 2-amino-7-hydroxy-4-(p-tolyl)-1,4 dihydroquinoline-3-carbonitrile (QUIN2), 2-amino-7-hydroxy-4-(4-methoxyphenyl)-1,4 dihydroquinoline-3 carbonitrile (QUIN3), 2-amino-4-(4-(dimethylamino)phenyl)-7-hydroxy-1,4-dihydroquinoline-3-carbonitrile (QUIN4).

2-amino-7-hydroxy-4-phenyl-1,4-dihydroquinoline-3-carbonitrile (QUIN1), 2-amino-7-hydroxy-4-(p-tolyl)-1,4 dihydroquinoline-3-carbonitrile (QUIN2), 2-amino-7-hydroxy-4-(4-methoxyphenyl)-1,4 dihydroquinoline-3 carbonitrile (QUIN3), 2-amino-4-(4-(dimethylamino)phenyl)-7-hydroxy-1,4-dihydroquinoline-3-carbonitrile (QUIN4) on carbon steel corrosion in aqueous phase. Experimental data shows that the corrosion inhibition follows the order: QUIN4 > QUIN3 > QUIN2 > QUIN1, which indicates that QUIN4 exhibits better inhibition performance among the studied inhibitors. Chemical efficiency of all inhibitors is investigated by the Density Functional Theory (DFT) methods and the adsorption energies of quinoline derivatives upon the Fe (1 1 0) surface is evaluated by Molecular Dynamics (MD) simulation. This study displays a good correlation between the theoretical and experimental data which confirms the reliability of the quantum chemical methods for studying the inhibition of corrosion of metal surfaces.

COMPUTATIONAL DETAILS

Quantum chemical calculations

Chemical properties of inhibitors were evaluated by quantum chemical calculations using the density functional theory (DFT) at the B3LYP-6-311++G** level of theory [7, 8] under the Gaussian 03 program [9]. The structure of four inhibitors was fully optimized,

and to confirm position of the optimized structures at minima (global or local) on the Potential Energy Surface (PES) their number of imaginary frequencies (NIMAG) was zero. The behavior of inhibitors is different in gas and aqueous phases. Hence, for a better comparison with experimental data, the effect of solvent (water) in the calculations was considered with Tomasi's Polarized Continuum Model (PCM) [10].

Total energy (E), Electronegativity (χ) and Global hardness (η) were calculated by applying the finite difference approximations for inhibitors from the following equations:

$$\eta = \frac{1}{2}\left[\frac{\partial^2 E}{\partial N^2}\right]_{v(r)} = \frac{I - A}{2} \quad (1)$$

$$\mu = -\chi = \left[\frac{\partial E}{\partial N}\right]_{v(r)} = \frac{I + A}{2} \quad (2)$$

Where *(r)*, μ, *I* and *A* are external potentials, chemical potentials, the ionization potential, and electron affinity, respectively. Also, according to the theorem of Koopmans, the ionization potential and electron affinity of a compound can be obtained as the energies of the frontier molecular orbitals (FMOs). Therefore, χ and η can be expressed as the following equations [11, 12]:

$$\eta = \frac{1}{2}\left(E_L - E_H\right) \quad (3)$$

$$\chi = -\frac{1}{2}\left(E_L + E_H\right) \quad (4)$$

Where E_H and E_L associated with the frontier molecular orbital HOMO and LUMO, respectively.

Global electrophilic index (ω) proposed by *Parr et al.* was calculated from the definitions of global hardness and the electronegativity as follows [13]:

$$\omega = \frac{\chi^2}{2\eta} \quad (5)$$

Value of ω shows electrophilicity of a compound. When the value of ω is low, compound is a good nucleophile and in high value of ω compound has a better electrophilicity. The total amount of electronic charge transferred, ΔN, from the inhibitor to surface of metal was calculated by the Pearson theory as follows [14]:

$$\Delta N = \frac{\chi_{Fe} - \chi_i}{2\left(\eta_{Fe} + \eta_i\right)} = \frac{\varphi_{Fe} - \chi_i}{2\left(\eta_{Fe} + \eta_i\right)} \quad (6)$$

Values of χ_{Fe} and η_{Fe} are theoretically 7 eV/mol and 0 eV/mol for bulk iron, respectively, due to metals are harder than the inhibitor's molecules. Some researchers proposed that because the work function (φ_m) of a metal surface is an appropriate measure of its electronegativity, so it should be used in the estimation of ΔN [15, 16]. In this study we had chosen Fe (1 1 0) surface, where the φ_m value obtained from DFT calculations is 4.82 eV [17].

The electric dipole polarizability (α) is inversely proportional to the third power of the hardness values [18, 19]. Therefore, molecule becomes more polarizable with increasing of softness. The following equation is used:

$$\alpha = -\left(\frac{\partial^2 E}{\partial^2 F_a \partial^2 F_b}\right) \qquad a, b = x, y, z \quad (7)$$

The mean polarizability (α) is calculated through the equation (8):

$$\alpha = \frac{1}{3}\left(\alpha_{xx} + \alpha_{yy} + \alpha_{zz}\right) \quad (8)$$

Fukui functions show the reactive centers within the molecules. For a molecule with N electrons functions can be expressed as follow:

$$F^+(r) = q_k(N) - q_k(N+1) \quad (9)$$

for atom k as an electrophile

$$F^-(r) = q_k(N-1) - q_k(N) \quad (10)$$

for atom k as a nucleophile

Where $q_k(N)$, $q_k(N+1)$, and $q_k(N-1)$ are the charges of the k_{th} atom for N, N + 1, and N - 1 electron systems, respectively.

Molecular Dynamics Simulation

A good method for considering the interaction between inhibitor and metal surface is Molecular Dynamics (MD) simulation. The interactions were investigated using the Forcite module of the Materials Studio 6.0 software developed by Accelrys Inc [20].

The interaction between Fe (110) surface and inhibitor molecules is carried out in a simulation box

(37.23×37.23×88.11Å) with periodic boundary conditions. A vacuums slab of 50 Å height is kept over the Fe (1 1 0) surface. Non-bonding, van der Waals and electrostatic interactions were used by the Ewald summation method with a cutoff radius of 15.50 Å [21]. All atoms in the Fe (110) surface were fixed and inhibitors were allowed to interact with it freely in the simulation process. The force field used is a COMPASS (condensed phase optimized molecular potentials for atomistic simulation studies) force field. Also, water and hydrogen chloride molecules for constructing a more reliable system were inserted to the solution layer in the simulated system. The liquid phase consists of 400 H_2O molecules, 5Cl^- ions, 5 H_3O^+ ions, and a single dissolved inhibitor molecule. The MD simulation is performed at 298.0K under canonical ensemble (NVT) using a time step of 1.0 fs and simulation time of 50 ps. the geometry of the system was optimized so that the total energy of the system was at a local minimum with respect to potential energy. Then, the dynamic process was followed to the equilibrium of the temperature and the energy. The interaction energy between the metal and the inhibitors were calculated according to the following equation [21]:

$$E_{int} = E_{(total)} - (E_{surface} + E_{inhibitor} + E_{solution}) \quad (14)$$

RESULTS AND DISCUSSION

The global molecular reactivity was investigated *via* analysis of the Frontier Molecular Orbitals (FMO) in terms of the interaction between the frontier orbitals, involving the HOMO and the LUMO [22]. According to frontier orbital theory, the inhibitors mainly interact on the Highest Occupied Molecular Orbital (HOMO) and Lowest unoccupied molecular orbital (LUMO). Inhibitors that can donate electrons to unoccupied *d* orbitals of metal surfaces and can also accept free electrons from the metal surface are good candidates for corrosion inhibitors. E_{HOMO} describes the electron donating ability of the molecule. Therefore, the higher the HOMO energy of the inhibitor, the greater the trend of offering electrons to an appropriate acceptor with a low empty molecular orbital energy. On the other hand, the energy of LUMO denotes the ability of the molecule to accept electrons using π^* orbitals to form π -back bonds. The lower value of E_{LUMO}, the easier the acceptance of electrons from metal surface. The inhibition efficiency increases with increasing HOMO energy level and decreasing LUMO energy level [23]. Table 1 present the calculated values of E_{HOMO} and E_{LUMO} for the studied quinoline derivatives. It is clear that E_{HOMO} in case of QUIN4 is highest which enhance the assumption that QUIN4 will adsorb more strongly on iron surface than other inhibitors. From Table 1, it can be concluded that the trend obtained for E_{LUMO}, that the capability of accepting electrons obey the order: QUIN1>QUIN2>QUIN3>QUIN4. This is not compatible well with the result (inhibition efficiencies) obtained from the experiments.

Global hardness (η) measures the resistance of an atom to a charge transfer [24]; So, harder inhibitors tend to show lower reactivity and greater stability, unlike the softer ones that readily undergo changes in electron density during interaction with metals. Pearson expressed the hard and soft acid and base (HSAB) principle [25, 26]. Corrosion inhibitors can be viewed from the HSAB principle and described as hard, soft, or borderline inhibitors. In accordance with the HSAB principle, hard acids form complexes with hard bases and soft acids form complexes with soft bases. Borderline acids form complexes with either soft or hard bases. In the research of corrosion inhibition chemistry, bulk iron is considered as soft acid, this would imply that the softest bases inhibitors are most effective for corrosion of these metals. As indicated in Table 1, the values of global hardness are according to the experimentally determined inhibition efficiency. Electronegativity (χ)[27] can be expressed with the equation (4) and electronegativity values studied inhibitors are listed in Table 1. From Table 1, we can see that, among quinoline derivatives, QUIN4 compound show lower χ, this effect increases donating an electron to the metallic surface. The term electrophilicity (ω) measures the electron-attracting power of chemical species for a molecular system. According to the definition, this index plays a fundamental role in determining the flow of electrons between metal surface and inhibitors. An inhibitor with a high ω value will naturally be more disposed to accepting electrons. A good electrophile is characterized by a high value of ω and contrariwise a good nucleophile is characterized by lower value of ω. For this reason, a molecule that have large nucleophilicity value is a good corrosion inhibitor while a molecule that have large electrophilicity value is

Table 1: Theoretical quantities calculated at the B3LYP/6311++G** level for the studied quinoline derivatives in aqueous phase.

	E_{HOMO} (ev)	E_{LUMO} (ev)	η (ev)	χ (ev)	ω (ev)	ΔN (e)	α (a.u.)	MV (cm^3/mol)	Surface area(cm^2/mol)
QUIN1	-5.77	-1.07	2.351	3.42	2.49	0.29	298.60	774.3	538.23
QUIN2	-5.76	-1.04	2.359	3.40	2.45	0.30	317.11	826.39	515.81
QUIN3	-5.74	-1.01	2.369	3.37	2.40	0.31	323.63	850.35	498.27
QUIN4	-5.39	-0.96	2.214	3.17	2.28	0.37	356.33	905.78	467.8

ineffective against corrosion. In our present study, QUIN4 is a stronger nucleophile than other inhibitors.

Using the work function, φ_{Fe} value of 4.82 eV for Fe (1 1 0) surfaces and global hardness, η_{Fe} value of 0 eV/mol for iron atom, the fraction of electrons transferred from quinoline derivatives to the iron surface, was calculated. Another parameter which is used in the corrosion inhibition studies is ΔN. According to Lukovits' s study [28], if $\Delta N < 3.6$, the inhibition efficiency increased by increasing the electron donor property of inhibitor. The obtained values of ΔN tabulated in Table 1 are all below 3.6 and the results show that the electron donor substitution in QUIN4 leads to increase in ΔN value. In this study, the fraction of electrons transferred of quinoline derivatives are positive then the studied inhibitors were the donor of electrons, and the carbon steel surface was the acceptor.

Molecular Volume (MV) and surface area values of the molecules illustrate possible metal surface coverage by the inhibitor. Large MV and surface area values for inhibitors can be attributed to more coverage of the metal surface. The corrosion rate decreases as the volume and surface area of the molecules increases due to the enhancement of large protection the metal surface. A comparison of the MV and surface area values support that the trend in the MV and surface area values are compatible well with the experimentally determined inhibition efficiencies. Polarizability is the ratio of induced dipole moment to the intensity of the electric field. The induced dipole moment is proportional to polarizability and reactivity indication [23]. High values of polarizability facilitate the strong adsorption process of corrosion inhibitors onto the metal surface and hence, high inhibition efficiency. The polarizabilities were evaluated using equation (8) for the two inhibitors. As can be seen, the polarizabilities are in the order QUIN4 > QUIN3 > QUIN2 > QUIN1, which correlates well with the corrosion inhibition efficiency observed. Local reactivity was discussed to analysis active sites of inhibitor molecules, due to estimate the exact active atoms of inhibitor molecules. The local indices such as natural atomic charge, distribution of frontier molecular orbital and Fukui functions are commonly used to analysis the behavior of the active sites of inhibitor molecules. Charges of atoms for the studied inhibitors in solution phase are listed in Tables 2, 3, 4 and 5, which were calculated using population analysis with atomic charge assignments produced according to the ChelpG scheme [29, 30].

It was found that the N_{15} and N_{19} atoms have the highest negative charge in studied inhibitors, then these sites will preferably react as an electron donor. The total negative charge (TNC) is obtained by summing up the negative charges on atoms of the inhibitors [31, 32]. TNC of the four inhibitors on Fe and Fe_2O_3 surface is listed in Table 6. It is clear from Table 6 that QUIN3 (-5.88) has the highest TNC value. Other parameters that were considered are the total number of charge centers (negative and positive). The negative and positive charge centers show donating and accepting electrons in inhibitor. Higher total number of charge centers of QUIN4 (see Table 6) indicated that chemical bond between QUIN4 and iron surface stronger than other quinoline derivatives and iron surface. The electron density distribution of the HOMO and LUMO orbitals are shown in Fig. 2. The HOMO electron density distribution indicates the reactive sites of the inhibitors that have a tendency to donate electrons to electrophilic species whereas the LUMO electron density distribution predicts the regions of the molecule with high tendency to accept electrons from nucleophilic species. In QUIN1, QUIN2 and QUIN3 inhibitors, the HOMO is localized on N15, N19, C2, C11, N13 and C6 atoms while in QUIN4, the HOMO is distributed on N15, N19, C11, C21, C22, N33 and C25 atoms. In QUIN1 and QUIN2, the LUMO is distributed around the entire molecule while in QUIN3

Table 2: The calculated Fukui functions and charge for the selected atoms of the QUIN1 inhibitor.

QUIN1	N	N+1	N-1	F^+	F^-
1 C	0.425	0.419	0.409	0.016	-0.006
2 C	-0.437	-0.383	-0.511	0.073	0.054
3 C	0.399	0.316	0.401	-0.002	-0.082
4 C	-0.288	-0.101	-0.332	0.044	0.186
5 C	-0.048	-0.104	-0.069	0.021	-0.056
6 C	-0.349	-0.238	-0.414	0.065	0.110
7 H	0.201	0.217	0.179	0.022	0.015
8 C	0.467	0.176	0.515	-0.047	-0.290
9 H	0.095	0.135	0.072	0.023	0.040
10 H	0.166	0.177	0.138	0.028	0.010
11 C	-0.620	-0.184	-0.737	0.116	0.435
12 C	0.669	0.563	0.653	0.015	-0.105
13 N	-0.606	-0.422	-0.681	0.074	0.183
14 H	0.410	0.430	0.413	-0.002	0.019
15 N	-0.919	-0.817	-1.013	0.093	0.102
16 H	0.433	0.445	0.416	0.016	0.011
17 H	0.425	0.425	0.421	0.004	-0.001
18 C	0.485	0.393	0.487	-0.002	-0.091
19 N	-0.654	-0.466	-0.771	0.117	0.187
20 C	0.088	0.105	0.093	-0.004	0.017
21 C	-0.239	-0.217	-0.282	0.042	0.022
22 C	-0.200	-0.200	-0.239	0.038	0.0001
23 C	-0.028	-0.028	-0.048	0.020	0.0001
24 H	0.124	0.137	0.107	0.016	0.012
25 C	-0.043	-0.032	-0.066	0.023	0.010
26 H	0.081	0.093	0.072	0.009	0.012
27 C	-0.164	-0.142	-0.211	0.046	0.022
28 H	0.089	0.101	0.073	0.016	0.012
29 H	0.098	0.108	0.080	0.017	0.010
30 H	0.108	0.116	0.084	0.023	0.007
31 O	-0.613	-0.588	-0.634	0.020	0.024
32 H	0.463	0.472	0.453	0.009	0.009
33 H	-0.020	0.090	-0.061	0.041	0.110

Table 3: The calculated Fukui functions and charge for the selected atoms of the QUIN2 inhibitor.

QUIN2	N	N+1	N-1	F^+	F^-
1 C	0.4227	0.413	0.409	0.013	-0.008
2 C	-0.437	-0.380	-0.5158	0.077	0.057
3 C	0.391	0.305	0.397	-0.005	-0.085
4 C	-0.286	-0.097	-0.339	0.053	0.189
5 C	-0.055	-0.112	-0.072	0.016	-0.057
6 C	-0.337	-0.224	-0.406	0.069	0.112
7 H	0.203	0.218	0.182	0.021	0.014
8 C	0.538	0.239	0.608	-0.070	-0.299
9 H	0.097	0.137	0.074	0.023	0.040
10 H	0.161	0.171	0.133	0.028	0.010
11 C	-0.642	-0.203	-0.769	0.126	0.439
12 C	0.686	0.573	0.672	0.013	-0.112
13 N	-0.620	-0.430	-0.701	0.080	0.190
14 H	0.414	0.433	0.417	-0.003	0.018
15 N	-0.926	-0.822	-1.022	0.096	0.104
16 H	0.434	0.446	0.417	0.016	0.011
17 H	0.426	0.425	0.422	0.004	-0.001
18 C	0.488	0.398	0.491	-0.002	-0.089
19 N	-0.653	-0.468	-0.774	0.120	0.185
20 C	0.039	0.059	0.037	0.002	0.019
21 C	-0.232	-0.209	-0.274	0.042	0.022
22 C	-0.177	-0.179	-0.205	0.028	-0.001
23 C	-0.142	-0.141	-0.165	0.022	0.001
24 H	0.137	0.150	0.120	0.017	0.013
25 C	-0.161	-0.149	-0.190	0.028	0.012
26 H	0.084	0.098	0.076	0.008	0.013
27 C	0.130	0.151	0.099	0.030	0.021
28 H	0.112	0.123	0.099	0.013	0.010
29 H	0.127	0.137	0.112	0.015	0.009
30 O	-0.615	-0.589	-0.637	0.021	0.025
31 H	0.464	0.473	0.454	0.009	0.008
32 H	-0.049	0.063	-0.096	0.047	0.113
33 C	-0.234	-0.251	-0.222	-0.012	-0.016
34 H	0.073	0.081	0.062	0.010	0.008
35 H	0.071	0.078	0.054	0.016	0.007
36 H	0.069	0.078	0.052	0.017	0.009

Table 4: The calculated Fukui functions and charge for the selected atoms of the QUIN3 inhibitor.

QUIN3	N	N+1	N-1	F^+	F^-
1 C	0.419	0.411	0.406	0.012	-0.008
2 C	-0.436	-0.378	-0.519	0.082	0.057
3 C	0.392	0.306	0.398	-0.005	-0.085
4 C	-0.308	-0.123	-0.372	0.063	0.185
5 C	-0.063	-0.117	-0.079	0.016	-0.054
6 C	-0.327	-0.219	-0.402	0.075	0.108
7 H	0.203	0.218	0.179	0.023	0.014
8 C	0.625	0.327	0.719	-0.094	-0.298
9 H	0.097	0.137	0.071	0.026	0.039
10 H	0.159	0.170	0.129	0.030	0.010
11 C	-0.652	-0.217	-0.788	0.136	0.434
12 C	0.669	0.562	0.650	0.018	-0.106
13 N	-0.626	-0.440	-0.711	0.085	0.185
14 H	0.418	0.437	0.423	-0.004	0.019
15 N	-0.909	-0.805	-1.007	0.098	0.103
16 H	0.428	0.439	0.409	0.018	0.011
17 H	0.424	0.423	0.419	0.005	-0.001
18 C	0.479	0.390	0.480	-0.001	-0.089
19 N	-0.651	-0.466	-0.779	0.127	0.185
20 C	-0.008	0.014	-0.015	0.007	0.023
21 C	-0.231	-0.209	-0.267	0.036	0.022
22 C	-0.153	-0.155	-0.169	0.016	-0.001
23 C	-0.187	-0.184	-0.208	0.020	0.003
24 H	0.144	0.158	0.126	0.017	0.013
25 C	-0.222	-0.208	-0.246	0.024	0.013
26 H	0.093	0.105	0.088	0.005	0.011
27 C	0.345	0.365	0.324	0.021	0.019
28 H	0.129	0.138	0.120	0.008	0.009
29 H	0.134	0.145	0.118	0.015	0.010
30 O	-0.615	-0.591	-0.638	0.022	0.024
31 H	0.464	0.473	0.454	0.010	0.008
32 H	-0.070	0.042	-0.124	0.053	0.113
33 O	-0.417	-0.409	-0.429	0.012	0.007
34 C	0.158	0.152	0.164	-0.006	-0.006
35 H	0.056	0.061	0.049	0.006	0.005
36 H	0.018	0.024	0.011	0.007	0.005
37 H	0.019	0.023	0.012	0.006	0.004

Table 5: The calculated Fukui functions and charge for the selected atoms of the QUIN4 inhibitor.

QUIN4	N	N+1	N-1	F^+	F^-
1 C	0.426	0.424	0.415	0.010	-0.001
2 C	-0.432	-0.395	-0.523	0.090	0.037
3 C	0.392	0.350	0.404	-0.011	-0.042
4 C	-0.310	-0.251	-0.388	0.077	0.058
5 C	-0.045	-0.055	-0.060	0.015	-0.010
6 C	-0.351	-0.324	-0.437	0.085	0.026
7 H	0.199	0.206	0.173	0.026	0.006
8 C	0.583	0.419	0.699	-0.115	-0.164
9 H	0.095	0.113	0.066	0.028	0.018
10 H	0.165	0.172	0.134	0.031	0.006
11 C	-0.633	-0.431	-0.779	0.145	0.202
12 C	0.673	0.624	0.658	0.015	-0.048
13 N	-0.616	-0.547	-0.708	0.092	0.069
14 H	0.412	0.420	0.418	-0.005	0.008
15 N	-0.926	-0.852	-1.030	0.104	0.074
16 H	0.431	0.434	0.412	0.019	0.002
17 H	0.427	0.423	0.423	0.004	-0.004
18 C	0.475	0.424	0.474	0.001	-0.051
19 N	-0.651	-0.563	-0.784	0.133	0.087
20 C	-0.028	0.092	-0.035	0.006	0.121
21 C	-0.203	-0.194	-0.227	0.024	0.008
22 C	-0.142	-0.152	-0.157	0.014	-0.009
23 C	-0.222	-0.125	-0.236	0.014	0.097
24 H	0.131	0.156	0.120	0.011	0.025
25 C	-0.251	-0.166	-0.266	0.015	0.084
26 H	0.077	0.102	0.072	0.005	0.024
27 C	0.312	0.287	0.301	0.010	-0.024
28 H	0.130	0.142	0.123	0.007	0.011
29 H	0.149	0.163	0.139	0.009	0.014
30 O	-0.617	-0.609	-0.640	0.022	0.008
31 H	0.464	0.469	0.454	0.010	0.004
32 H	-0.059	0.002	-0.119	0.059	0.061
33 N	-0.385	-0.192	-0.408	0.023	0.193
34 C	0.058	-0.026	0.073	-0.015	-0.084
35 H	0.060	0.094	0.053	0.007	0.033
36 H	0.022	0.075	0.012	0.009	0.053
37 H	0.020	0.071	0.013	0.007	0.050
38 C	0.091	-0.009	0.114	-0.022	-0.100
39 H	0.008	0.061	0.001	0.008	0.053
40 H	0.011	0.067	0.001	0.010	0.056
41 H	0.054	0.094	0.045	0.009	0.039

Table 6: The interaction energy obtained from MD simulation for adsorption of inhibitors on Fe (1 1 0) surface. the Total Negative Charge (TNC), the total number of the Negative Charge Centers(NCC) and the Positive Charge Centers(PCC) of the studied inhibitors in aqueous phase calculated at the B3LYP/6311++G** level.

system	$E_{interaction(Fe\text{-}inhibitor)}$ (kcal/mol)	$E_{interaction(Fe2O3\text{-}inhibitor)}$ (kcal/mol)	TNC(ev)	NCC	PCC
QUIN1	-2153.911	-3613.61	-5.235	14	18
QUIN2	-2228.575	-3658.03	-5.575	15	21
QUIN3	-2254.756	-3682.06	-5.882	16	21
QUIN4	-2289.001	-3738.18	-5.879	16	25

and QUIN4 the LUMO is localized on C23, C1, C25, C21, C5, and C4 atoms. The electron density distribution of the frontier orbitals are in good agreement with the results of partial charges.

Tables 2, 3, 4 and 5 show condensed Fukui indices, the atoms of the molecule which accepting electrons have more $F^{+}(r)$ (the index for nucleophilic attack); when the atoms of molecule which donating electrons have more $F^{-}(r)$ (the index for electrophilic attack for an inhibitor molecule). It is clear that the preferred site for nucleophilic and electrophilic attack for the four inhibitors are C11 atoms, which indicated that these atoms will be the most probable nucleophilic and electrophilic reactive sites during the absorption.

In spite of advancements in quantum chemical techniques, due to computationally expensive for systems involving a large number of molecules, Molecular dynamics (MD) simulation usually only applied to these systems. Many corrosion inhibition studies nowadays contain the use of molecular dynamics simulation as an important tool in understanding the interaction between adsorbate-metal surfaces [32-35]. As the adsorption energy is negatively affected, the metal-adsorbent interaction becomes stronger [36]. In this study, four selected inhibitors were placed on the Fe (1 1 0) and Fe_2O_3 (1 1 0) surfaces. To examine the equilibrium state of systems, diagrams of temperature and energy obtained via MD simulations were analyzed. The Figs. 3 and 4 show temperature and energy fluctuation curve as a function of time. Fluctuations of the temperature are in a range of 298 ± 5 K and the fluctuations of energy are less than 0.5%, indicating that the system has reached an equilibrium state [37]. The system equilibrium state and the best adsorption configurations of the surface-adsorbed inhibitor are depicted in Fig. 5.

Interaction energy, which results from the binding of the inhibitor to iron surface, was calculated to measure the stability of inhibitor-Fe (1 1 0) complexes. The values of the interaction energies of the four inhibitors on Fe (1 1 0) and Fe_2O_3 (1 1 0) surfaces are listed in Table 6. It is clear from Table 6 that QUIN4 has higher negative interaction energy as compared to the other inhibitor. Therefore, the adsorption of QUIN4 on the iron surface in aqueous solution is easier than other inhibitors. Also, the values of negative interaction energy for four inhibitors suggests that the adsorption on mild steel and iron oxide surface is spontaneous. Moreover, the interaction energy between the inhibitor molecules and Fe_2O_3 (1 1 0) surface is lower than Fe (1 1 0) surface. It means that the inhibitor molecules can easily absorb on Fe_2O_3 surface and protect it from corrosion. Indeed, the presence of oxide layer on the iron surface can encourage the adsorption of the inhibitor molecules on the surface, mainly via electrostatic attractive forces.

CONCLUSIONS

Inhibition efficiencies of four quinoline derivatives have been studied on corrosion of carbon steel using quantum chemical parameters and molecular dynamics (MD) simulation method in the aqueous phase. The results obtained are summarized below:

a) Among quinoline derivatives, QUIN4 compound showed lower χ, this effect increases donating an electron to the metallic surface.

b) QUIN4 was the stronger nucleophile than other inhibitors.

c) The electron donor substitution in QUIN4 led to an increase in ΔN value.

d) The fraction of electrons transferred of quinoline derivatives are positive then the studied inhibitors

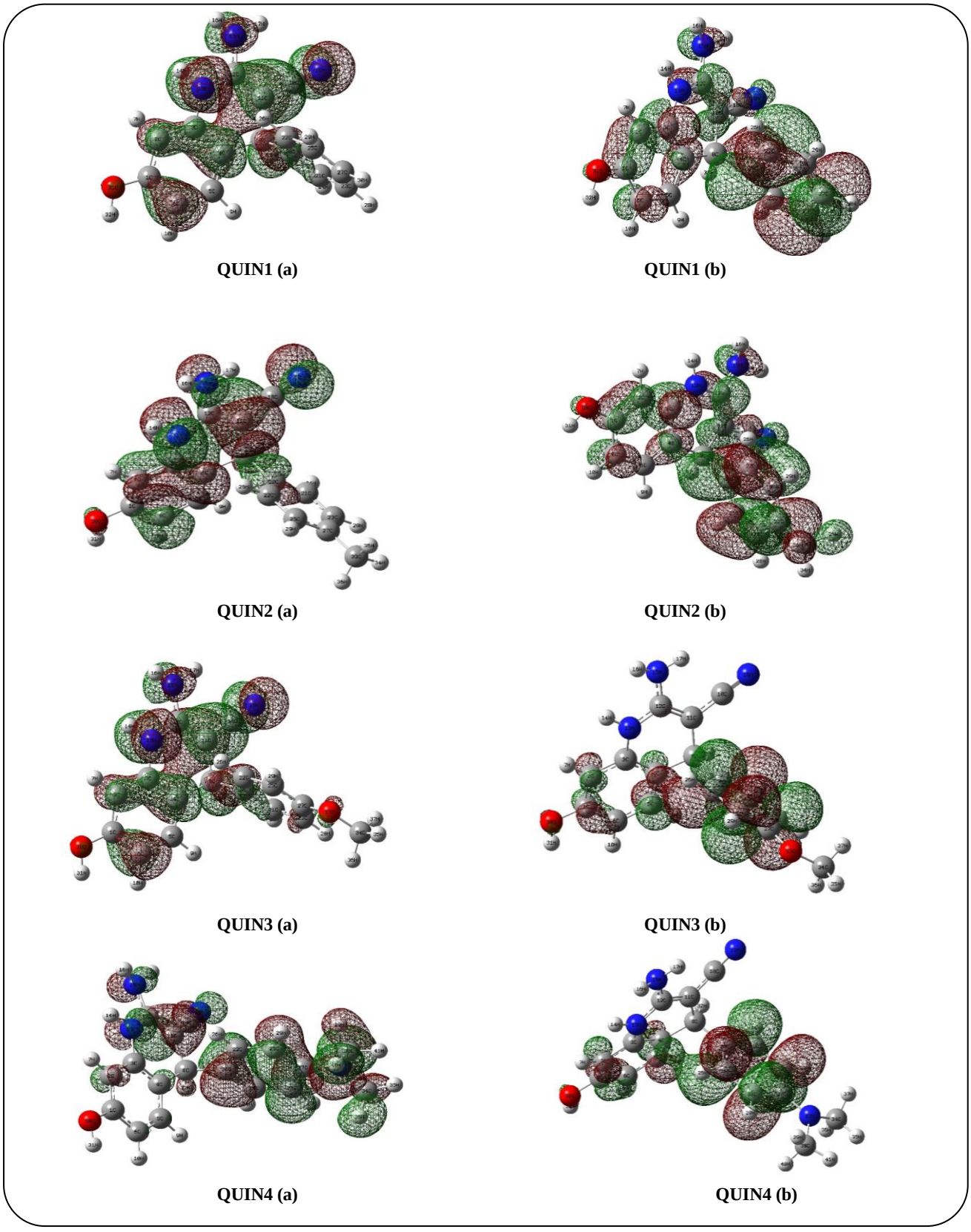

Fig. 2: The frontier molecule orbital density distribution of the investigated inhibitors: (a) HOMO, (b) LUMO.

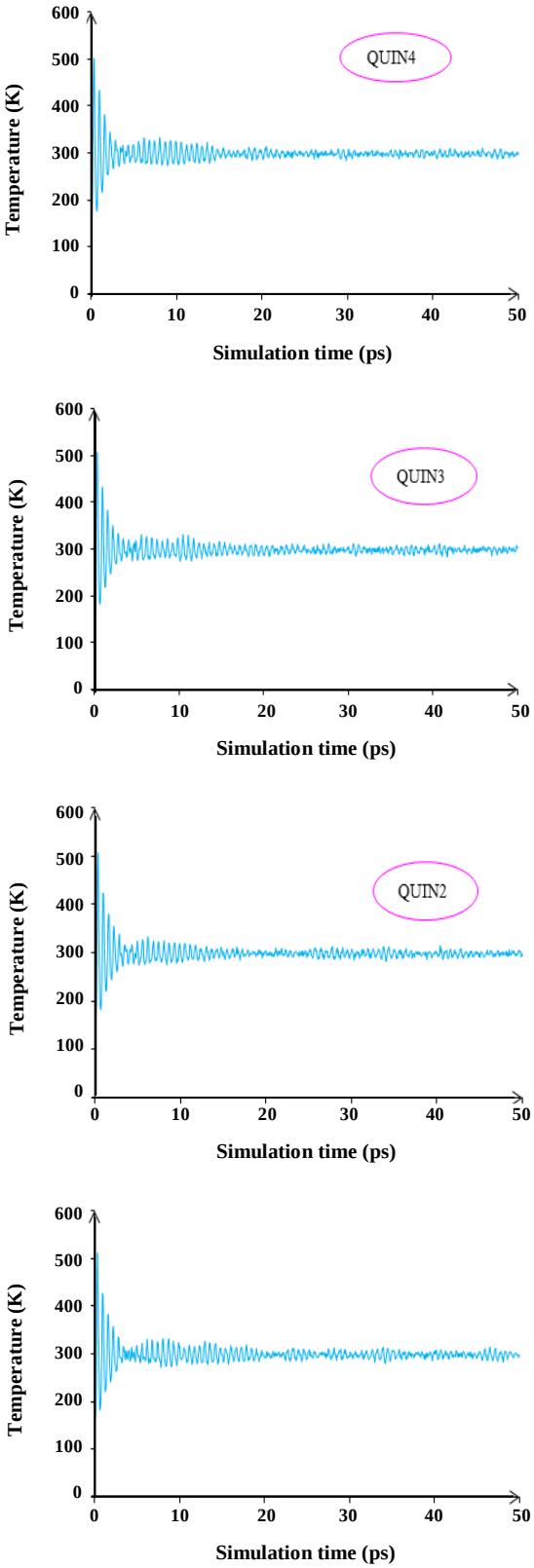

Fig. 3: Temperature equilibrium curve obtained from molecular dynamics simulation for quinoline derivatives.

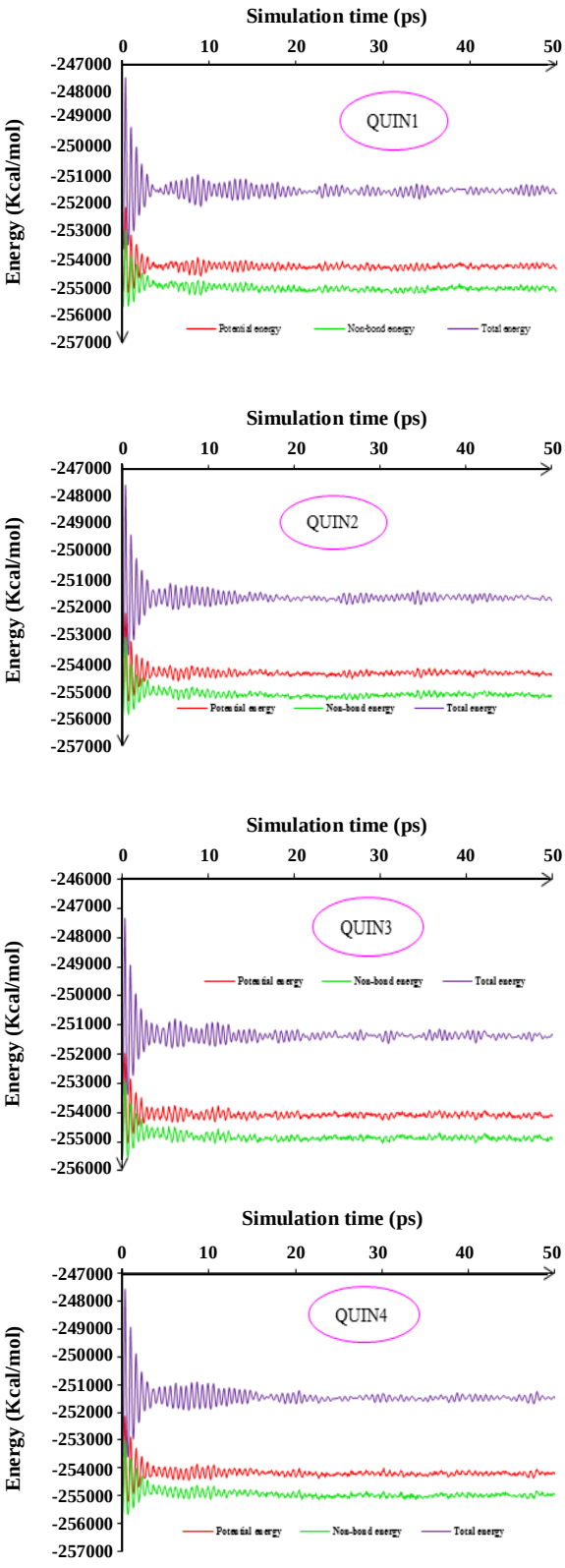

Fig. 4: Energy fluctuant curve obtained from molecular dynamics simulation for quinoline derivatives.

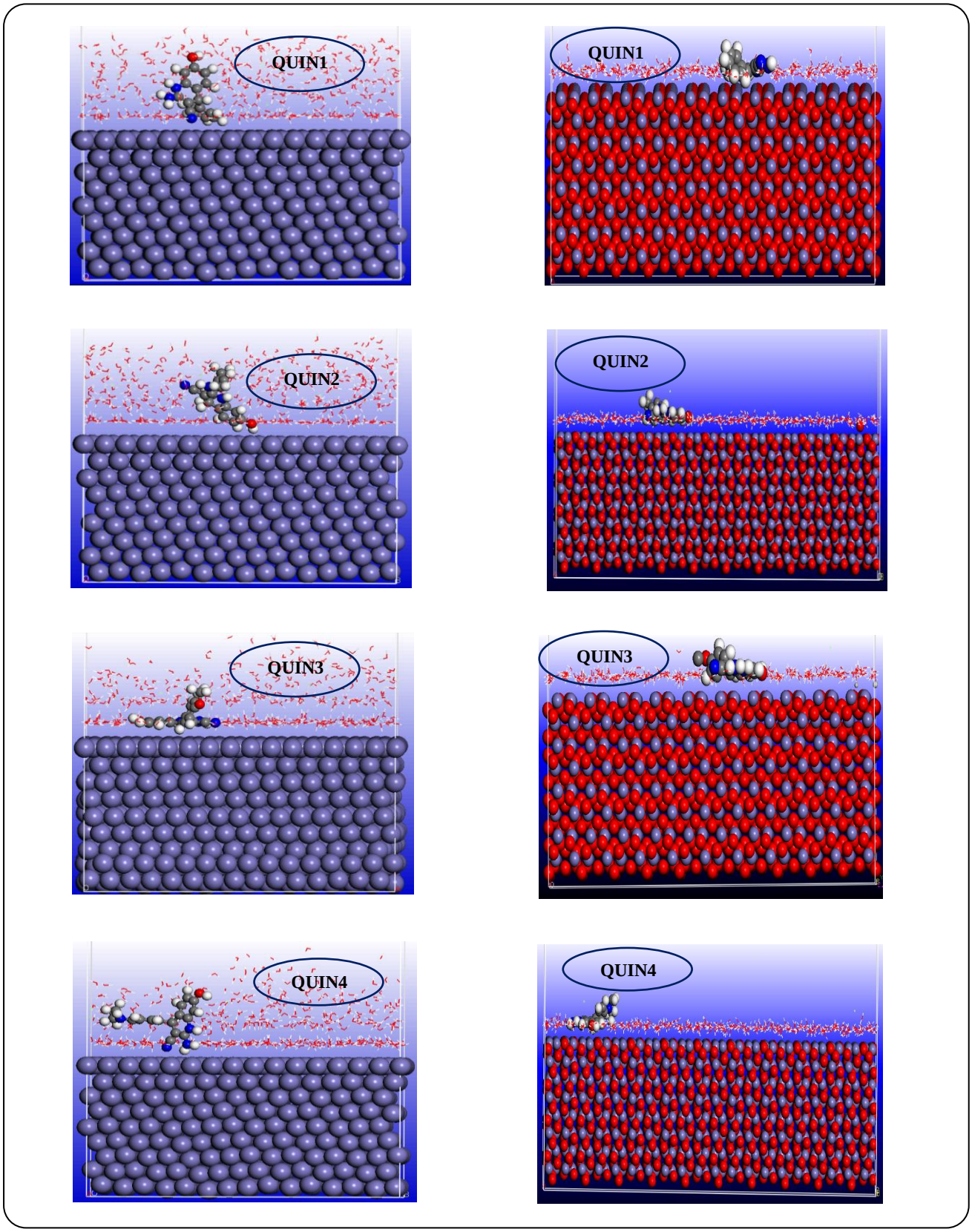

Fig. 5: Equilibrium adsorption configurations of quinoline derivatives on Fe (1 1 0) (left) and Fe_2O_3 (1 1 0) (right) surfaces.

were the donor of electrons, and the carbon steel surface was the acceptor.

e) The polarizabilities are in the order QUIN4 > QUIN3 > QUIN2 > QUIN1, which correlates well with the corrosion inhibition efficiency observed.

f) Higher total number of charge centers of QUIN4 indicated that the chemical bond between QUIN4 and iron surface stronger than other quinoline derivatives and iron surface.

g) The electron density distribution of the frontier orbitals is in good agreement with the results of partial charges.

h) Fluctuations of the temperature are in a range of 298 ± 5 K and the fluctuations of energy are less than 0.5%, indicating that the system has reached an equilibrium state.

i) Values of negative interaction energy for four inhibitors suggests that the adsorption on mild steel surface is spontaneous.

In brief, results of DFT and MD simulations calculations confirm that QUIN4 has more inhibition efficiency than other derivatives, which is in good agreement with the experimental inhibition efficiency data reported. Therefore, DFT along with MD successfully used as reliable approaches to screen organic corrosion inhibitors prior to experimental validation.

Acknowledgment

We gratefully acknowledge the support provided by the Kerman-Branch, Islamic Azad University.

Received : Jul. 23, 2017 ; Accepted : Jan. 1, 2018

REFERENCES

[1] Swiler T.P., Loehman R.E., Molecular Dynamics Simulations of Reactive Wetting in Metal–Ceramic Systems, *Acta Materialia*, **48**: 4419-4424 (2000).

[2] Kornherr A., French S.A., Sokol A.A., Catlow C.R.A., Hansal S., Hansal W.E.G., Besenhard J.O., Kronberger H., Nauer G.E., Zifferer G., Interaction of Adsorbed Organosilanes with Polar Zinc Oxide Surfaces: a Molecular Dynamics Study Comparing Two Models for the Metal Oxide Surface, *Chem. Phys. Lett.*, **393**: 107-111 (2004).

[3] Shahraki M., Dehdab M., Elmi Sh., Theoretical Studies on the Corrosion Inhibition Performance of Three Amine Derivatives on Carbon Steel: Molecular Dynamics Simulation and Density Functional Theory Approaches, *J. Taiwan Inst. Chem. Eng.*, **62**: 313–321 (2016).

[4] Dehdab M., Shahraki M., Habibi-Khorassani S.M., Theoretical Study of Inhibition Efficiencies of Some Amino Acids on Corrosion of Carbon Steel in Acidic Media: Green Corrosion Inhibitors, *Amino Acides*, **48(**1): 291–306 (2015).

[5] Dehdab M., Shahraki M., Habibi-Khorassani S.M., Inhibitory Effect of Some Benzothiazole Derivatives on Corrosion of Mild Steel: A Computational Study, *Iran. J. Sci. Technol.*, **39A**(3): 311-324 (2015).

[6] Masoud M.S., Awad M.K., Shaker M.A., El-Tahawy M.M.T., The Role of Structural Chemistry in the Inhibitive Performance of some Aminopyrimidines on the Corrosion of Steel, *Corrosion Scien*ce, **52**: 2387-2396 (2010).

[7] Becke A. D., Density-Functional Exchange-Energy Approximation with Correct Asymptotic Behavior, *Phys. Rev. A*, **38**:3098-3100 (1988).

[8] Becke A.D., Density-Functional Thermochemistry. III. The Role of Exact Exchange, *J. Chem. Phys.*, **98**:5648-5652 (1993).

[9] M.J.T. Frisch G.W., Schlegel H.B., Scuseria G.E., Robb M.A., Cheeseman J.R., Montgomery Jr. J.A., Vreven T., Kudin K.N., Burant J.C., Millam J.M., Iyengar S.S., Tomasi J., Barone V., Mennucci B., Cossi M., Scalmani G., Rega N., Petersson G. A., Nakatsuji H., Hada M., Ehara M., Toyota K., Fukuda R., Hasegawa J., Ishida M., Nakajima T., Honda Y., Kitao O., Nakai H., Klene M., Li X., Knox J.E.; Hratchian H.P., Cross J.B., Bakken V., Adamo C., Jaramillo J., Gomperts R., Stratmann R.E., Yazyev O., Austin A.J., Cammi R., Pomelli C., Ochterski J.W., Ayala P.Y., Morokuma K., Voth G.A., Salvador P., Dannenberg J.J., Zakrzewski V.G., Dapprich S., Daniels A.D., Strain M.C., Farkas O., Malick D.K., Rabuck A.D., Raghavachari K., Foresman J.B., Ortiz J.V., Cui Q., Baboul A.G., Clifford S., Cioslowski J., Stefanov B.B., Liu G., Liashenko A., Piskorz P., Komaromi I., Martin R.L., Fox D.J., Keith T., Al-Laham M.A., Peng C. Y., Nanayakkara A.,

Challacombe M., Gill P.M.W., Johnson B., Chen W., Wong M.W., Gonzalez C., Pople J.A., Gaussian 03, Revision C.02 (Gaussian, Inc., Wallingford CT), (2004).

[10] Miertuš S., Scrocco E., Tomasi J., Electrostatic Interaction of a Solute with a Continuum. A Direct Utilizaion of AB initio Molecular Potentials for the Prevision of Solvent Effects, *Chem. Phys.*, **55**: 117-129 (1981).

[11] Koopmans T., Über die Zuordnung von Wellenfunktionen und Eigenwerten zu den Einzelnen Elektronen Eines Atoms, *Physica*, **1**:104-113 (1934).

[12] Zhan C.G., Nichols J.A., Dixon D.A., Ionization Potential, Electron Affinity, Electronegativity, Hardness, and Electron Excitation Energy: Molecular Properties from Density Functional Theory Orbital Energies, *J. Phys. Chem. A.*, **107**:4184-4195 (2003).

[13] Parr R.G., Szentpály L.V., Liu S., Electrophilicity Index, *J Am. Chem. Soc*., **121**:1922-1924 (1999).

[14] Maynard A.T., Huang M., Rice W.G., Covell D.G., Reactivity of the HIV-1 Nucleocapsid Protein p7 Zinc Finger Domains from the Perspective of Density-Functional Theory, *Proceedings of the National Academy of Sciences of the United States of America*, **95**:11578-11583 (1998).

[15] Pearson R.G., Absolute Electronegativity and Hardness: Application to Inorganic Chemistry, *Inorg. Chem.*, **27**:734-740 (1988).

[16] Khaled K.F., Studies of Iron Corrosion Inhibition Using Chemical, Electrochemical and Computer Simulation Techniques, *Electrochimica Acta*, **55**: 6523-6532 (2010).

[17] Kokalj A., On the HSAB Based Estimate of Charge Transfer between Adsorbates and Metal Surfaces, *Chem. Phys.*, **393**:1-12 (2012).

[18] Zevallos J., Toro-Labbé A., A Theoretical Analysis of the Kohn-Sham and Hartree-Fock Orbitals and Their Use in the Determination of Electronic Properties, *J. Chil. Chem. Soc.*, **48**:39-47 (2003).

[19] Ghanty T.K., Ghosh S.K., Correlation between Hardness, Polarizability, and Size of Atoms, Molecules, and Clusters, *J. Phys. Chem.*, **97**:4951-4953 (1993).

[20] Materials Studio 6.1 Manual. San Diego, CA: Accelrys, Inc; (2007).

[21] Satoh S., Fujimoto H., Kobayashi H., Theoretical Study of NH3 Adsorption on Fe(110) and Fe(111) Surfaces, *J. Phys. Chem. B*, **110**:4846-4852 (2006).

[22] Fukui K., The Role of Frontier Orbitals in Chemical-Reactions, *Angew. Chem. Int. Ed.*, **21**:801-809 (1982).

[23] Ebenso E.E., Arslan T., Kandemirli F., Caner N., Love I., Quantum Chemical Studies of some Rhodanine Azosulpha Drugs as Corrosion Inhibitors for Mild Steel in Acidic Medium, *Int. J. Quantum Chem*, **110**:1003-1018 (2010).

[24] Parr R.G., Yang W., "Density Functional Theory of Atoms and Molecules", Oxford University Press, Oxford (1989).

[25] Pearson R.G., Hard and Soft Acids and Bases, HSAB, Part 1: Fundamental Principles, *Journal of Chemical Education*, **45**:581-585 (1968).

[26] Habibi-Khorassani S.M., Shahraki M., Noroozifar M., Darijani M., Dehdab M., Yavari Z., Inhibition of aluminum corrosion in acid solution by environmentally friendly antibacterial corrosion inhibitors: Experimental and theoretical investigations, *Prot. Met. Phys. Chem*, **53(3)**:579-590 (2017).

[27] Yadav M., Kumar S., Bahadur I., Ramjugernath D., Corrosion Inhibitive Effect of Synthesized Thiourea Derivatives on Mild Steel in a 15% HCl Solution, *Int. J. Electrochem. Sci.*, **9**:6529 – 6550 (2014).

[28] Lukovits I., Kalman E., Zucchi F., DFT Calculations for Corrosion Inhibition of Ferrous Alloys by Pyrazolopyrimidine Derivatives, *Corrosion*, **57**:3-8 (2001).

[29] Breneman C.M., Wiberg K.B., Determining Atom-Centered Monopoles from Molecular Electrostatic Potentials. The Need for High Sampling Density in Formamide Conformational Analysis, *J. Comput. Chem*., **11**: 361-373 (1990).

[30] Shahraki M., Habibi-Khorassani S. M., Noroozifar M., Yavari Z., Darijani M. Dehdab M., Corrosion Inhibition of Copper in Acid Medium by Drugs: Experimental and Theoretical Approaches, *Iranian Journal of Materials Science and Engineering*., **14**:35-47 (2017).

[31] Nataraja S.E., Venkatesha T.V., Tandon H.C., Computational and Experimental Evaluation of the Acid Corrosion Inhibition of Steel by Tacrine, *Corrosion Science*, **60**:214-223 (2012).

[32] Karima A., Sihem A., Jean-Pierre M., Inhibition of Copper Corrosion by Ethanolamine in 100 ppm NaCl, *Iran. J. Chem. Chem. Eng. (IJCCE)*, **35**(4): 89-98 (2016).

[33] Xia S., Qiu M., Yu L., Liu F., Zhao H., Molecular Dynamics and Density Functional Theory Study on Relationship between Structure of Imidazoline Derivatives and Inhibition Performance, *Corrosion Science*, **50**:2021-2029 (2008).

[34] Tang Y., Yao L., Kong C., Yang W., Chen Y., Interfacial Reactions between Molten Al and a Co–Cr–Mo Alloy with and Without Oxidation Treatment, *Corrosion Science*., **53**:2046-2049 (2011).

[35] Feng L., Yang H., Wang F., Experimental and Theoretical Studies for Corrosion Inhibition of Carbon Steel by Imidazoline Derivative in 5% NaCl Saturated $Ca(OH)_2$ Solution, *Electrochimica Acta*., **58**:427-436 (2011).

[36] Khaled K.F., Evaluation of Electrochemical Frequency Modulation as a New Technique for Monitoring Corrosion and Corrosion Inhibition of Carbon Steel in Perchloric Acid Using Hydrazine Carbodithioic Acid Derivatives, *J. Appl. Electrochem*., **41**:423-433 (2011).

[37] Zeng J., Zhang J., Gong X., Molecular Dynamics Simulation of Interaction between Benzotriazoles and Cuprous Oxide Crystal, *Comput. Theor. Chem.*, **963**:110-114 (2011).